A Finite Annular Plate Element with Slight Deviation for Vibration Analysis of a Nearly Axisymmetric Disk*

Jintai CHUNG**, Min Joong KIM***
and Jang Moo LEE***

Vibration of a nearly axisymmetric disk is analyzed by using a newly developed finite annular plate element with slight deviation from axisymmetry. Even if the developed annular plate element has four degrees of freedom, the annular element can contain the effects of slight deviation in density, stiffness or thickness. To provide validity of the proposed annular element, the natural frequencies of disks with deviation are computed by the finite element method using the new annular elements and the convergence and accuracy of the natural frequencies are investigated. It is shown that, when a disk has slight deviation, the finite element method using the proposed elements is more efficient to compute the natural frequencies and the mode shapes compared to a commercial code. Furthermore, the effects of deviation on the dynamic characteristics are also analyzed. Finally, it is evaluated how much deviation is acceptable for the proposed method to result in reliable computations.

Key Words: Nearly Axisymmetric Disk, Finite Annular Plate Element with Deviation, Vibration

1. Introduction

Vibration of structures deviating from perfect axisymmetry is an interesting topic. Many practical machine parts and structural components have non-axisymmetry such as ribs, grooves and concentrated weights to ensure adequate stiffness, rigidity, balance, or noise control. This deviation from axisymmetry is sometimes significant and obviously related to the dynamic characteristics of a structure.

Numerous articles about elastic imperfections, flaws, and cracks on nearly axisymmetric structures have appeared. During the late 1970's and early 1980's, some useful vibration information was offered about annular plates having non-concentric interior circumferential boundaries[1),(2)] and non-uniform axisymmetric plates having varying thickness[3),(4)]. In the recent literature, the subject has extended to non-axisymmetric plates such as V-notched plates[5] or various practical elements[6]. The influence of structural imperfection on thin-walled structures was introduced in Godoy[7]. He showed that small imperfections may introduce changes in the stresses due to the loads. Mote and his co-workers[8),(9)] studied circular plates with small asymmetry in various conditions. A perturbation approach to the vibration analysis of finite solids containing small elastic imperfections was proposed by Shen and Mote[9]. They investigated the effect of edge slots and small inhomogeneous elastic inclusions on the eigenvalues of annular plates. On the other hand, Hong and Lee[10] presented an analytical method to predict the effects of local deviation on the free in-plane vibration of nearly axisymmetric rings. Recently, Chung and Lee[11] developed a new finite ring element to analyze the natural frequencies and modes of a nearly axisymmetric shell structure with local deviation. However, since this element is applicable only to a nearly axisymmetric shell structure with local deviation, it is required to develop a finite annu-

* Received 10th December, 2001
** Department of Mechanical Engineering, Hanyang University, 1271 Sa-1-dong, Ansan, Kyunggi-do 425-791, Republic of Korea. E-mail: jchung@hanyang.ac.kr
*** Department of Mechanical Design and Production Engineering, Seoul National University, San-56-1, Shinlim-dong, Kwanak-Ku, Seoul 151-742, Republic of Korea

lar plate element that can be used in the transverse vibration analyses of a disk with slight deviation.

In this paper, a new finite annular plate element with slight deviation is developed to analyze dynamic characteristics of a nearly axisymmetric disk and the applicability of the finite annular plate element is verified. The annular plate element is able to consider the effects of slight deviation, even though the element has the same active degrees of freedom as the conventional axisymmetric element. By using the developed elements, the equation of motion in matrix-vector form is obtained for disks with slight deviation. The convergence and accuracy are checked for natural frequencies computed by using the present method. A study is also carried out on the effects of the deviation from axisymmetry on the natural frequencies and mode shapes. Furthermore, it is evaluated how much amount of deviation is acceptable for the proposed method to result in reliable computations.

2. Finite Annular Plate Element with Slight Deviation

Consider a nearly axisymmetric annular disk with slight deviation. The deviation may be classified into the density, stiffness and thickness deviations. A region with deviation is different from the other normal region in material properties or dimensions such as density, Young's modulus and thickness. Figure 1 demonstrates that the deviation shape can be divided by point and line deviations. When a nearly axisymmetric disk is discretized by finite annular plate elements, the finite annular plate elements are constructed as shown in Fig. 2, where an annular plate e is defined by two adjacent nodal circles e and $e+1$. Although the proposed annular plate element has only two nodal circles, the deviation from axisymmetry can be considered in the element. Figure 3 shows schematics of the annular elements with deviation. The element is defined by the dimensions of the average radius R, the thickness h and the width ΔR and the material properties are given by the mass density ρ, Young's modulus E and Poisson's ratio ν. The position and size of the deviated part are specified by θ_d, $\Delta\theta$ and h_d, while the material properties are given by ρ_d, E_d and ν_d. When a disk has slight deviation, meshes using the conventional elements and the proposed elements are presented in Fig. 4.

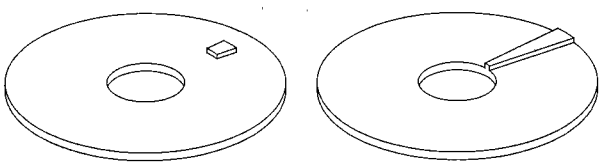

Fig. 1 Examples of nearly axisymmetric disks with slight deviation: (a) point deviation and (b) line deviation

The transverse displacement w at a point in the annular plate element of Fig. 3 may be represented by

$$w(t, r, \theta)=W_0+\sum_{n=1}^{N} W_n(t, r)\cos n\theta + \sum_{n=1}^{N} \overline{W}_n(t, r)\sin n\theta \quad (1)$$

where n is the circumferential mode number, that is, the number of the nodal diameters and N is the total number of the basis functions. W_n and $\overline{W}_n$ of Eq.(1) can be approximated by cubic polynomials of r:

$$W_n=\alpha_1+\alpha_2 r+\alpha_3 r^2+\alpha_4 r^3,$$
$$\overline{W}_n=\bar{\alpha}_1+\bar{\alpha}_2 r+\bar{\alpha}_3 r^2+\bar{\alpha}_4 r^3 \quad (2)$$

where α_i and $\bar{\alpha}_i$ are functions of time to be deter-

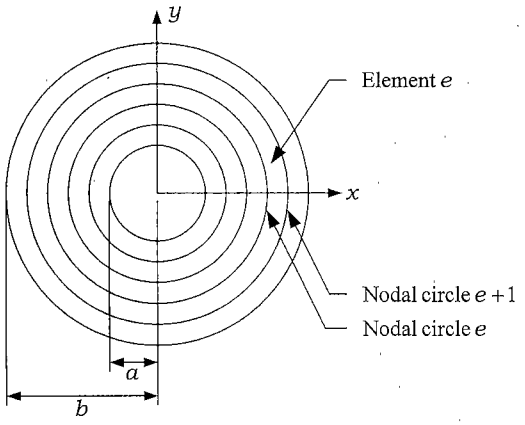

Fig. 2 Construction of the finite annular plate elements

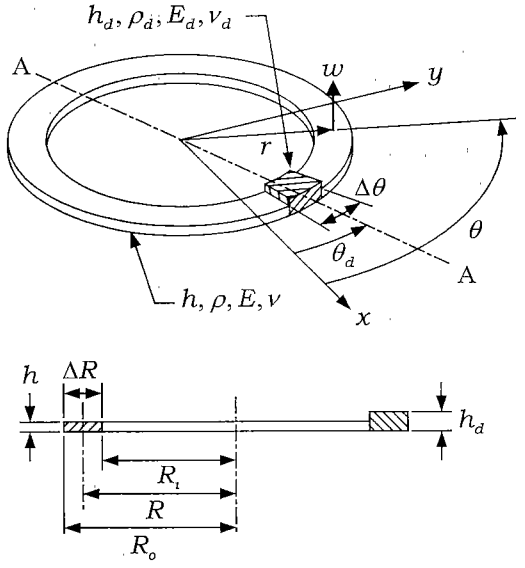

Cross - section A-A

Fig. 3 Schematics of the finite annular plate elements with deviation

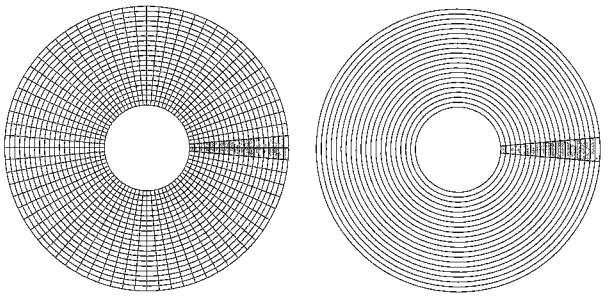

(a) (b)

Fig. 4 Meshes for a nearly axisymmetric disk with slight deviation: (a) the conventional elements and (b) the proposed elements

mined. Equations (1) and (2) imply that the transverse displacement in an element is periodic with respect to θ and its behaviour is like the displacement of a beam in the r direction.

It is assumed, in this paper, that the mode shapes of an annular plate element are already known even when the annular element has slight deviation. The theoretical background can be found in Hong and Lee[10]. They showed that the natural modes of a ring with slight deviation are separated into symmetric and asymmetric ones. The deviated part is located on the anti-nodal point of the symmetric mode while it is located on the nodal point of the asymmetric mode. This means that the asymmetric mode shape rotates with $\pi/2n$ from the symmetric mode shape for each circumferential mode number n. For example, the asymmetric mode shape rotates with 45° from the symmetric one for $n=2$.

Considering the mode rotation due to the local deviation, both the symmetric and asymmetric modes of an annular plate element may be expressed by

$$w=(\alpha_1+\alpha_2 r+\alpha_3 r^2+\alpha_4 r^3)\cos(n\theta-\pi\beta/2) \quad (3)$$

where β is a parameter related to the symmetric and asymmetric modes. $\beta=0$ is for the symmetric mode while $\beta=1$ is for the asymmetric mode. Denoting the transverse displacement and the slope at nodal circle e, i.e., at $r=R_i$ by w_e and $(\partial w/\partial r)_e$, respectively, the transverse modes in element e can be expressed in terms of the displacements and slopes at the nodal circles e and $e+1$. That is, the mode shapes for w may be written by

$$w=\boldsymbol{N}^T\boldsymbol{w}_e\cos(n\theta-\pi\beta/2) \quad (4)$$

where $\boldsymbol{N}$ is the 4×1 shape function vector and $\boldsymbol{w}_e$ is the 4×1 nodal displacement vector. These two vectors are given by

$$\boldsymbol{N}^T=\{1, r, r^2, r^3\}\begin{bmatrix}1 & R_i & R_i^2 & R_i^3\\ 0 & 1 & 2R_i & 3R_i^2\\ 1 & R_o & R_o^2 & R_o^3\\ 0 & 1 & 2R_o & 3R_o^2\end{bmatrix}^{-1},$$

$$\boldsymbol{w}_e=\begin{Bmatrix} w_e\\ (\partial w/\partial r)_e\\ w_{e+1}\\ (\partial w/\partial r)_{e+1}\end{Bmatrix} \quad (5)$$

Here, it should be noted that the shape function vector $\boldsymbol{N}$ is a function of r and the nodal displacement vector $\boldsymbol{w}_e$ is a function of time.

Adopting the Kirchhoff plate theory, the curvature change vector

$$\kappa=\{\kappa_r, \kappa_\theta, 2\kappa_{r\theta}\}^T \quad (6)$$

is expressed in terms of the transverse displacement w. In Eq.(6), the curvature changes, κ_r and κ_θ, and the surface twist, $\kappa_{r\theta}$, are given by

$$\kappa_r=-\frac{\partial^2 w}{\partial r^2},\quad \kappa_\theta=-\frac{1}{r^2}\frac{\partial^2 w}{\partial\theta^2}-\frac{1}{r}\frac{\partial w}{\partial r},$$

$$\kappa_{r\theta}=-\frac{1}{r}\frac{\partial^2 w}{\partial r\partial\theta}+\frac{1}{r^2}\frac{\partial w}{\partial\theta} \quad (7)$$

Substituting Eq.(4) into Eq.(7), the curvature change vector of Eq.(6) can be written in terms of the nodal displacement vector:

$$\kappa=\boldsymbol{\Theta}\boldsymbol{B}\boldsymbol{w}_e \quad (8)$$

where

$$\boldsymbol{\Theta}=\begin{bmatrix}\cos(n\theta-\pi\beta/2) & 0 & 0\\ 0 & \cos(n\theta-\pi\beta/2) & 0\\ 0 & 0 & \sin(n\theta-\pi\beta/2)\end{bmatrix},\quad \boldsymbol{B}=\begin{bmatrix}-d^2\boldsymbol{N}^T/dr^2\\ n^2\boldsymbol{N}^T/r^2-d\boldsymbol{N}^T/rdr\\ 2nd\boldsymbol{N}^T/rdr-2n\boldsymbol{N}^T/r^2\end{bmatrix} \quad (9)$$

Note that the 3×3 diagonal matrix $\boldsymbol{\Theta}$ is related to the mode rotation and the 3×4 matrix $\boldsymbol{B}$ is a function of r.

The stresses in an annular plate element are expressed in terms of the strains and the elasticity matrix. For a flexible annular disk, the stress couples and the curvature changes have a relationship of

$$\boldsymbol{m}=\boldsymbol{D}\kappa \quad (10)$$

where $\boldsymbol{m}$ is the stress couple vector and $\boldsymbol{D}$ is the elasticity matrix. These matrices may be written as

$$\boldsymbol{m}=\{m_r, m_\theta, m_{r\theta}\}^T,\quad \boldsymbol{D}=D\begin{bmatrix}1 & \nu & 0\\ \nu & 1 & 0\\ 0 & 0 & (1-\nu)/2\end{bmatrix} \quad (11)$$

in which m_r, m_θ and $m_{r\theta}$ are the couples per unit length of the disk middle surface and $D=Eh^3/12(1-\nu^2)$ is the flexible rigidity. Note that the elasticity matrix $\boldsymbol{D}$ may become a function of θ because the thickness, Young's modulus and Poisson's ratio of a disk with deviation can change with the angular position θ.

3. Equation of Motion in Matrix-Vector Form

The equation of motion for the free vibration of a

disk with deviation can be derived from Hamilton's principle given by

$$\delta\int_{t_1}^{t_2}(T-U)\mathrm{d}t=0 \tag{12}$$

where T and U are the kinetic and strain energies, respectively; t_1 and t_2 are arbitrary time; δ is the variation operator. Suppose that a disk is discretized into N annular plate elements and the variation operator is independent of integration with respect to time, Eq.(12) can be rewritten as

$$\sum_{e=1}^{N}\int_{t_1}^{t_2}(\delta T_e-\delta U_e)\mathrm{d}t=0 \tag{13}$$

where T_e and U_e are the kinetic and strain energies of element e.

The kinetic energy of an annular plate element is given by

$$T_e=\frac{1}{2}\int_{V_e}\rho\left(\frac{\partial w}{\partial t}\right)^2\mathrm{d}V \tag{14}$$

where V_e is the volume of element e. Taking the variation for Eq.(14), integrating the equation by parts with respect to time, and then substituting Eq.(4) into the resultant equation, the following equation is obtained:

$$\int_{t_1}^{t_2}\delta T_e\mathrm{d}t=-\int_{t_1}^{t_2}\delta\boldsymbol{w}_e^T\boldsymbol{M}_e\ddot{\boldsymbol{w}}_e\mathrm{d}t \tag{15}$$

where $\boldsymbol{M}_e$ is the element mass matrix defined by

$$\boldsymbol{M}_e=\int_{V_e}\rho\boldsymbol{N}\boldsymbol{N}^T\cos^2(n\theta-\pi\beta/2)\mathrm{d}V \tag{16}$$

The infinitesimal volume $\mathrm{d}V$, shown in Fig. 3, can be written as

$$\mathrm{d}V=r\,\mathrm{d}\theta\cdot\mathrm{d}s\cdot\mathrm{d}h=\left(R+\frac{\Delta R}{2}\xi\right)d\theta\cdot\frac{\Delta R}{2}\mathrm{d}\xi\cdot\mathrm{d}h \tag{17}$$

where ξ is a parametric defined by $\xi=2s/L-1$. Substituting Eq.(17) into Eq.(16), the element mass matrix may be expressed as

$$\boldsymbol{M}_e=\frac{\rho_e\Delta R}{2}\int_{-1}^{1}\left(R+\frac{\Delta R}{2}\xi\right)\boldsymbol{N}\boldsymbol{N}^T\mathrm{d}\xi \tag{18}$$

where

$$\rho_e=\pi\rho h+\frac{1}{2}\left[\Delta\theta+\frac{(-1)^\beta\sin n\Delta\theta}{n}\right](\rho_d h_d-\rho h) \tag{19}$$

in which ρ_d and h_d are the density and thickness of the deviated portion of the element while ρ and h are density and thickness of the normal portion, respectively.

On the other hand, the element strain energy is represented by

$$U_e=\frac{1}{2}\int_{A_e}\boldsymbol{m}^T\boldsymbol{\kappa}\,\mathrm{d}A \tag{20}$$

where A_e is the middle surface area of element e. Similarly to the procedure in deriving Eq.(15), taking the variation of Eq.(20) and using Eqs.(8) and (10), the time integration for the variation of the element strain energy can be written by

$$\int_{t_1}^{t_2}\delta U_e\mathrm{d}t=\int_{t_1}^{t_2}\delta\boldsymbol{w}_e^T\boldsymbol{K}_e\boldsymbol{w}_e\,\mathrm{d}t \tag{21}$$

in which the element stiffness matrix $\boldsymbol{K}_e$ is defined by

$$\boldsymbol{K}_e=\int_{A_e}\boldsymbol{B}^T\boldsymbol{\Theta}\boldsymbol{D}\boldsymbol{\Theta}\boldsymbol{B}\mathrm{d}A \tag{22}$$

The infinitesimal area $\mathrm{d}A$ is expressed as

$$\mathrm{d}A=r\,\mathrm{d}\theta\cdot\mathrm{d}s=\left(R+\frac{\Delta R}{2}\xi\right)d\theta\cdot\frac{\Delta R}{2}\mathrm{d}\xi \tag{23}$$

Introduction Eq.(23) into Eq.(22) yields

$$\boldsymbol{K}_e=\frac{\Delta R}{2}\int_{-1}^{1}\left(R+\frac{\Delta R}{2}\xi\right)\boldsymbol{B}^T\boldsymbol{D}_e\boldsymbol{B}\mathrm{d}\xi \tag{24}$$

where

$$\boldsymbol{D}_e=\pi\boldsymbol{D}+\frac{1}{2}\left[\Delta\theta\boldsymbol{I}+\frac{(-1)^\beta\sin n\Delta\theta}{n}\boldsymbol{T}_K\right](\boldsymbol{D}_d-\boldsymbol{D}) \tag{25}$$

in which $\boldsymbol{I}$ is the 3 by 3 identity matrix, $\boldsymbol{D}_d$ and $\boldsymbol{D}$ are the elasticity matrices of the deviated part and the normal part, and $\boldsymbol{T}_K$ is given by

$$\boldsymbol{T}_K=\begin{bmatrix}1&0&0\\0&1&0\\0&0&-1\end{bmatrix} \tag{26}$$

Substitution of Eqs.(18) and (24) into Eq.(13) leads to

$$\sum_{e=1}^{N}\int_{t_1}^{t_2}\delta\boldsymbol{w}_e^T(\boldsymbol{M}_e\ddot{\boldsymbol{w}}_e+\boldsymbol{K}_e\boldsymbol{w}_e)\mathrm{d}t=0 \tag{27}$$

Equation (27) is valid for arbitrary variation $\delta\boldsymbol{w}$, so that assembling the element mass and stiffness matrices in the global mass and stiffness matrices yields the equation of motion in matrix-vector form:

$$\boldsymbol{M}\ddot{\boldsymbol{W}}+\boldsymbol{K}\boldsymbol{W}=\boldsymbol{0} \tag{28}$$

where $\boldsymbol{M}$ is the global mass matrix, $\boldsymbol{K}$ is the global stiffness matrix, and $\boldsymbol{W}$ is the global displacement vector given by

$$\boldsymbol{W}=\{w_1,(\partial w/\partial r)_1,w_2,(\partial w/\partial r)_2,\cdots,w_{N+1},(\partial w/\partial r)_{N+1}\}^T \tag{29}$$

4. Convergence and Accuracy

The natural frequencies are computed for an annular disk with the inner radius a and the outer radius b. This disk reduces to a circular disk when the inner radius is equal to zero, i.e., $a=0$. The natural frequencies and the corresponding mode shapes are obtained from the eigenvalue problem given by

$$(\boldsymbol{K}-\omega_n^2\boldsymbol{M})\boldsymbol{X}=\boldsymbol{0} \tag{30}$$

where ω_n is the natural frequency and $\boldsymbol{X}$ is the natural mode vector. To simplify discussion for the natural frequency, the following non-dimensional natural frequency λ_n is introduced:

$$\lambda_n=\omega_n b\sqrt{\rho h/D} \tag{31}$$

where b, h, ρ and D are the dimension and material properties for the non-deviated part of the disk. If there is no other specification on the material properties and dimensions for the disks, computations of this study use the data given by $\rho=2\,700\ \mathrm{kg/m^3}$, $E=$

Table 1 Convergence characteristics for the non-dimensional natural frequencies λ_n of an axisymmetric annular disk when the disk is free at both the inner and outer radii

N	Mode (m,n) (0, 2)	(1, 0)	(0, 3)	(1, 1)	(0, 4)	(1, 2)
10	5.0019	8.3701	12.499	18.326	22.183	33.008
20	4.9846	8.3764	12.456	18.374	22.099	33.020
30	4.9814	8.3776	12.448	18.383	22.083	33.022
40	4.9803	8.3780	12.445	18.386	22.078	33 022
50	4.9797	8.3782	12.444	18.388	22.075	33.023
60	4.9795	8.3783	12.443	18.389	22.074	33.023
70	4.9793	8.3784	12.442	18.389	22.073	33.023
80	4.9792	8.3784	12.442	18.390	22.073	33.023
ANSYS (7920 elements)	4.9804	8.3812	12.445	18.403	22.081	33.034

Table 2 Non-dimensional natural frequencies λ_n of a free axisymmetric circular disk with $\nu=0.33$ when the mode shapes have no nodal diameters, i.e., $n=0$

Mode (m,n)	Proposed method (80 elements)	Itao and Crandall [14]	Difference (%)
(0, 2)	9.071	9.068	0.03
(0, 3)	38.521	38.507	0.04
(0, 4)	87.855	87.813	0.05
(0, 5)	156.97	156.88	0.06
(0, 6)	245.86	245.70	0.07
(0, 7)	354.51	354.25	0.07
(0, 8)	482.93	482.55	0.08
(0, 9)	631.13	630.59	0.09
(0, 10)	799.09	798.37	0.09

7×10^{10} N/m^2, $\nu=0.27$, $h=10$ mm, $b=500$ mm and $a/b=0.3$.

It is necessary to check the convergence and accuracy of the natural frequencies of disks computed with the proposed finite annular plate elements. As the first example, the convergence of the natural frequencies for an axisymmetric annular disk is investigated when the disk is free at both the inner and outer radii. As shown in Table 1, the lowest six non-dimensional natural frequencies are converged as the number of elements N increases. In Table 1, mode (m, n) denotes a mode with m nodal circles and n nodal diameters. The natural frequencies are also computed by using 7920 SHELL63 elements, which are provided by a commercial code ANSYS[12]. The converged natural frequencies obtained from the proposed method are very close to the natural frequencies from ANSYS with 7920 elements. For a free axisymmetric circular disk with $a=0$ and $\nu=0.33$, another computation is carried out to guarantee accuracy of the natural frequencies. The computation results are summarized in Table 2, where the non-dimensional natural frequencies computed with 80 proposed elements are in good agreement with those given by Itao and Crandall[13].

Next, investigation is performed on computation accuracy of the finite element method using the new annular plate elements, when an annular disk has slight deviation from axisymmetry. For all computations, 80 finite annular plate elements are used in the present method, while 7920 SHELL63 elements are used for ANSYS, because the proposed method demands much fewer elements for accurate computation compared to ANSYS. In fact, the numbers of degrees of freedom are 160 and 24192 for the models of the proposed method and ANSYS, respectively. Hence, there is no need to compare their computation time. Table 3 shows the non-dimensional natural frequencies computed from the proposed method and ANSYS when an annular disk has only the density deviation of $\rho_d/\rho=2$. The deviation shape is defined by the line deviation with $\Delta\theta=10°$ as shown in Fig. 1 (b). Other dimensions and material properties of the deviated part are the same as the non-deviated part, namely, $E_d=E$, $\nu_d=\nu$ and $h_d=h$. The differences are very small between the non-dimensional natural frequencies computed by the proposed method and ANSYS, as demonstrated in Table 3, where subscripts s and a represent the symmetric and asymmetric modes respectively. Similarly, Table 4 illustrates the good agreement of the natural frequencies obtained from the present method and ANSYS when a disk only has the stiffness deviation of $E_d/E=2$.

Table 3 Non-dimensional natural frequencies λ_n of an annular disk with a density deviation of $\rho_d/\rho=2$ when the disk is free at both the inner and outer radii

Mode (m,n)	Proposed method (80 elements)	ANSYS (7920 elements)	Difference (%)
$(0, 2)_s$	4.8477	4.8562	−0.18
$(0, 2)_a$	4.9778	4.9789	−0.02
(1, 0)	8.2644	8.2654	−0.01
$(0, 3)_s$	12.117	12.151	−0.22
$(0, 3)_a$	12.434	12.438	−0.03
$(1, 1)_s$	17.900	17.909	−0.05
$(1, 1)_a$	18.388	18.402	−0.08
$(0, 4)_s$	21.506	21.593	−0.40
$(0, 4)_a$	22.048	22.056	−0.04
$(1, 2)_s$	32.151	32.160	−0.03
$(1, 2)_a$	33.014	33.025	−0.03

Table 4 Non-dimensional natural frequencies λ_n of an annular disk with a stiffness deviation of $E_d/E=2$ when the disk is free at both the inner and outer radii

Mode (m,n)	Proposed method (80 elements)	ANSYS (7920 elements)	Difference (%)
$(0, 2)_s$	5.0216	5.0153	0.13
$(0, 2)_a$	5.0720	5.0337	0.76
(1, 0)	8.4940	8.4499	0.52
$(0, 3)_s$	12.555	12.535	0.16
$(0, 3)_a$	12.669	12.580	0.70
$(1, 1)_s$	18.626	18.564	0.33
$(1, 1)_a$	18.658	18.597	0.32
$(0, 4)_s$	22.270	22.241	0.13
$(0, 4)_a$	22.479	22.323	0.69
$(1, 2)_s$	33.355	33.258	0.29
$(1, 2)_a$	33.601	33.396	0.61

5. Numerical Investigation and Discussion

The effects of deviation from axisymmetry on the natural frequencies are studied. In addition, it is assessed how much deviation is acceptable for the proposed approach to yield reliable computation results. A physical model for all computations is a free annular disk with deviation of which the shape is given by the line deviation with $\Delta\theta=10°$ as shown in Fig. 1(b). As with the previous computations in this paper, a finite element model for the present method has 80 annular plate elements while a model for ANSYS has 7920 SHELL63 elements. Three kinds of deviation are considered in this study: the density, stiffness and thickness deviations.

First, consider the case that the annular disk has only density deviation. For the various values for the density ratios of ρ_d/ρ, the non-dimensional natural frequencies of several modes are computed. These frequencies are presented in Fig. 5, where Figs. 5(a), (b), (c) and (d) represents the variation of the natural frequencies of modes (0, 2), (0, 3), (1, 1) and (1, 2). The circle and the square represent the symmetric and asymmetric modes respectively and the white and black symbols stand for the proposed method and ANSYS. Figure 5 demonstrates the fact that the natural frequencies are split into the symmetric and asymmetric mode frequencies when the disk has the density deviation. Although the differences between the natural frequencies computed from the proposed method and ANSYS are very small, they become large as the density of the deviated part increases. It is also noted that the natural frequencies computed from the present method are always less than those from ANSYS. Another interesting point is that, as the density deviation increases, the natural frequencies corresponding to the symmetric mode decrease while those corresponding to the asymmetric mode remain constant. The mode shapes corresponding to mode (1, 2) are shown in Fig. 6, when the annular disk possesses the density deviation of $\rho_d/\rho=2$. In Fig. 6, the part surrounded by the solid lines indicates the deviated part of the disk. Figures 6(a) and (b) are for the symmetric and asymmetric modes computed from the proposed method respectively while Figs. 6(c) and (d) are for the symmetric and asymmetric modes computed from ANSYS. It is observed that the mode shapes for the proposed method are nearly identical to those for ANSYS. Moreover, Fig. 6 illustrates that the symmetric mode shape is symmetric with respect to the deviated part but the asymmetric mode is not symmetric.

Secondly, the effects of the stiffness deviation on the natural frequencies of a free annular disk are investigated by using both the proposed method and ANSYS. A prominent point shown in Fig. 7 is that the natural frequencies for both the symmetric and asymmetric modes increase along with the stiffness of the

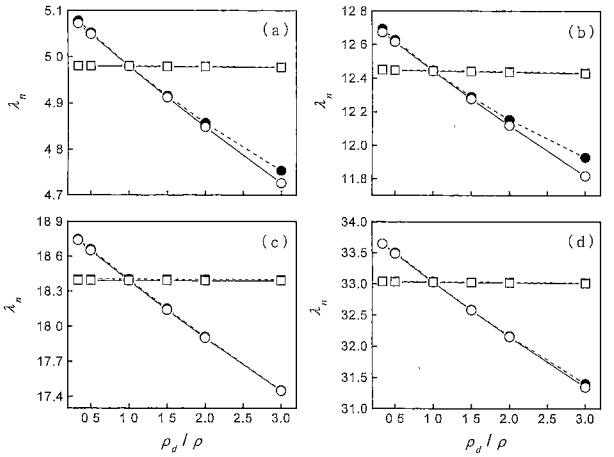

Fig. 5 Effects of the density deviation on the non-dimensional natural frequencies λ_n of a free annular disk for (a) mode (0, 2), (b) mode (0, 3), (c) mode (1, 1) and (d) mode (1, 2). ···■··· ANSYS (symmetric mode); —□— Present method (symmetric mode); ···●··· ANSYS (asymmetric mode); —○— Present method (asymmetric mode)

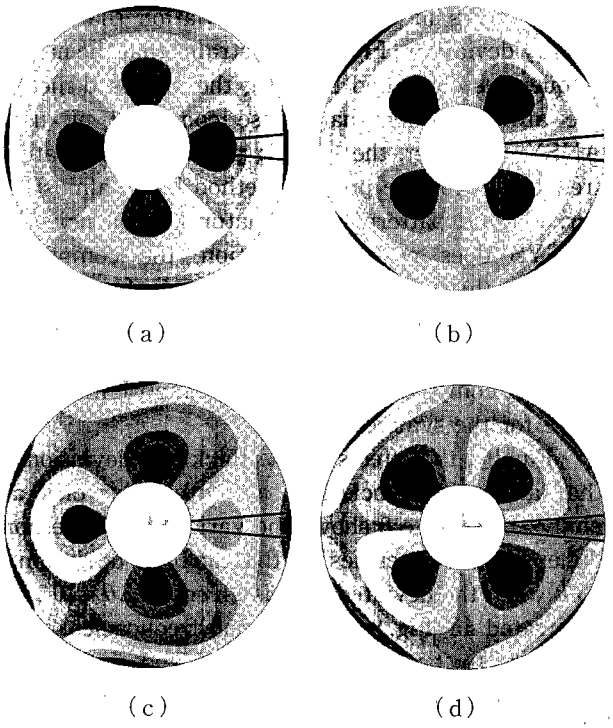

Fig. 6 Mode shapes of mode (1, 2) for an annular disk with the density deviation of $\rho_d/\rho=2$: (a) the symmetric mode computed by the proposed method, (b) the asymmetric mode computed by the proposed method, (c) the symmetric mode computed by ANSYS and (d) the asymmetric mode computed by ANSYS

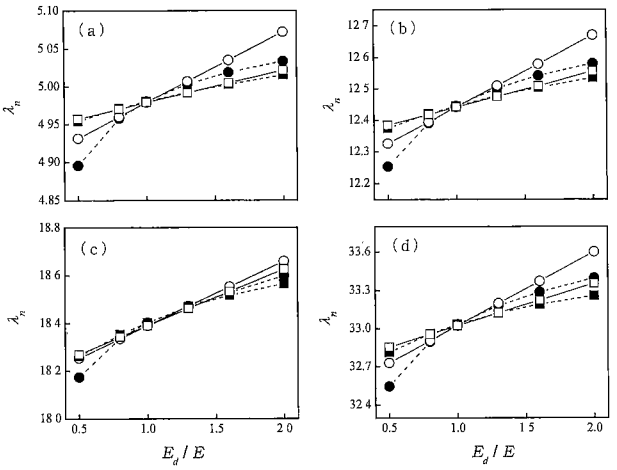

Fig. 7 Effects of the stiffness deviation on the non-dimensional natural frequencies λ_n of a free annular disk for (a) mode (0, 2), (b) mode (0, 3), (c) mode (1, 1) and (d) mode (1, 2). ···■··· ANSYS (symmetric mode); —□— Present method (symmetric mode); ···●··· ANSYS (asymmetric mode); —○— Present method (asymmetric mode)

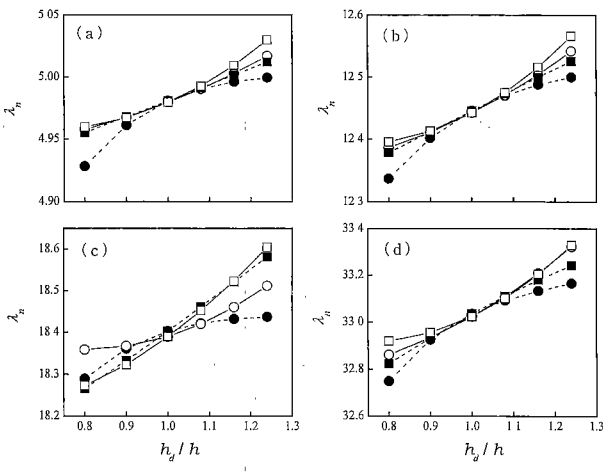

Fig. 8 Effects of the thickness deviation on the non-dimensional natural frequencies λ_n of a free annular disk for (a) mode (0, 2), (b) mode (0, 3), (c) mode (1, 1) and (d) mode (1, 2). ···■··· ANSYS (symmetric mode); —□— Present method (symmetric mode); ···●··· ANSYS (asymmetric mode); —○— Present method (asymmetric mode)

deviated part, namely, the value of E_d/E. The splitting phenomenon is also observed for the stiffness deviation similar to the density deviation. Regarding the computation accuracy, the new method exhibits larger errors in the stiffness deviation than in the density deviation. Figure 7 illustrates that the natural frequencies computed by using the proposed method are always larger than those computed by using ANSYS. In fact, the varying pattern of the natural frequencies for the present method looks almost linear, but the pattern of the natural frequencies for ANSYS does not. In addition, the comparison between the computation results of the proposed method and ANSYS shows that, when the stiffness deviation exists, the proposed method yields more accurate computations for the asymmetric mode than those for the symmetric mode.

Finally, the effects of the thickness deviation on the natural frequencies for a free annular disk are analyzed. Figure 8 shows the variations of the non-dimensional frequencies for the thickness deviation of h_d/h when the deviated part is given by $\Delta\theta=10°$. As illustrated in Fig. 8, the natural frequencies corresponding to both the symmetric and asymmetric modes increases with the thickness deviation h_d/h. This implies that the thickness deviation adds a larger stiffness effect to the disk rather than a mass effect. In other words, if the thickness increases in the deviated part, the stiffness of the disk increases more compared to the mass. From the viewpoint of computation, the present method yields poorer accuracy when the disk has the thickness deviation than when the disk has the density or stiffness deviations. However, if the deviated part, i.e., $\Delta\theta$ decreases, it is expected that the computation accuracy will be improved even for large thickness deviation.

6. Conclusions

The transverse vibration analysis of a nearly axisymmetric disk with slight deviation is performed by using newly developed finite annular plate elements with slight deviation from axisymmetry. For this kind of a disk, the finite element method using the developed elements is more efficient to compute the natural frequencies and mode shapes than a commercial code, because the proposed method needs much fewer elements to obtain the same level of accuracy than the commercial code. On the other hand, this study does not only analyze the deviation effects on the dynamic characteristics of a disk, but it is also evaluated how much amount of deviation is acceptable for the proposed method to yield reliable computations. Furthermore, the differences between the results of the present method and the commercial code are discussed. The other results of this study may be summarized as follows.

(1) The natural frequencies are split into two frequencies corresponding to the symmetric and asymmetric modes when slight deviation exists in a disk.

(2) The symmetric mode shape is symmetric with respect to the deviated part but the asymmetric mode is not symmetric.

(3) The differences of the natural frequencies between the symmetric and asymmetric modes

increase with the amount of deviation.

(4) The proposed method yields lower natural frequencies than ANSYS when a disk has density deviation. However, it results in higher frequencies than ANSYS when a disk has stiffness deviation.

(5) When density deviation exists in a disk, the natural frequencies corresponding to the symmetric mode decrease while those corresponding to the asymmetric mode remain constant.

(6) When a disk possesses stiffness or thickness deviation, the natural frequencies for both the symmetric and asymmetric modes increase with the stiffness or thickness of the deviated part.

(7) To obtain accurate computation results, application of the new method should be limited to a slight amount of deviation. In addition, the method produces more accurate computation results in the order of the density, stiffness and height deviation.

References

(1) Eastep, F.E. and Hemming, F.G., Estimation of Fundamental Frequency of Noncircular Plates with Free, Circular Cutouts, Journal of Sound and Vibration, Vol. 56 (1978), p. 155.

(2) Khurasia, H.B. and Rawtani, S., Vibration Analysis of Circular Plates with Eccentric Hole, ASME Journal of Applied Mechanics, Vol. 45 (1978), p. 215.

(3) Celep, Z., Free Vibration on Some Circular Plates of Arbitrary Thickness, Journal of Sound and Vibration, Vol. 70 (1980), p. 379.

(4) Selmane, A. and Lakis, A.A., Natural Frequencies of Transverse Vibrations of Non-uniform Circular and Annular Plates, Journal of Sound and Vibration, Vol. 220 (1999), p. 225.

(5) So, J., Leissa, A.W., Huang, C.S. and Kim, J.W., Vibrations of Circular Plates with Clamped V-notches or Rigidly Constrained Radial Cracks, Journal of Sound and Vibration, Vol. 181 (1993), p. 185.

(6) Vinayak, H. and Singh, R., Eigensolutions of Annular-like Elastic Disks with Intentionally Removed or Added Material, Journal of Sound and Vibration, Vol. 192 (1996), p. 741.

(7) Godoy, L.A., Thin-Walled Structures with Structural Imperfections: Analysis and Behavior, (1996), Pergamon, Oxford.

(8) Yu, R.C. and Mote, C.D., Vibration and Parametric Excitation in Asymmetric Circular Plates under Moving Loads, Journal of Sound and Vibration, Vol. 119 (1987), p. 409.

(9) Shen, I.Y. and Mote, C.D., Dynamic Analysis Containing Small Elastic Imperfections: Theory with Application to Asymmetric Plates, Journal of Sound and Vibration, Vol. 155 (1992), p. 443.

(10) Hong, J.S. and Lee, J.M., Vibration of Circular Rings with Local Deviation, ASME Journal of Applied Mechanics, Vol. 61 (1994), p. 317.

(11) Chung, J. and Lee, J.M., Vibration Analysis of an Nearly Axisymmetric Shell Structure using a New Finite Ring Element, Journal of Sound and Vibration, Vol. 219 (1999), p. 35.

(12) Swanson Analysis Co., ANSYS User's Manual, Version 5.1 (1996).

(13) Itao, K. and Crandall, S.H., Natural Mode and Natural Frequencies of Uniform, Circular, Free-edge Plate, ASME Journal of Applied Mechanics, Vol. 46 (1979), p. 448.